Pseudogap in the microwave response of YBa$_2$Cu$_3$O$_{7-x}$

M R Trunin, Yu A Nefyodov and A F Shevchun

Institute of Solid State Physics RAS, 142432 Chernogolovka, Moscow district, Russia

Abstract
The in-plane and out-of-plane surface impedance and microwave conductivity components of YBa$_2$Cu$_3$O$_{7-x}$ ($0.07 \leqslant x \leqslant 0.47$) single crystal are determined in the wide ranges of temperature T and carrier concentration p in CuO$_2$ planes. The following features of the superfluid density $n_s(T, p) \propto \lambda_{ab}^{-2}(T, p)$ are observed at $T < T_c/2$ and $0.078 \leqslant p \leqslant 0.16$: (i) $n_s(0, p)$ depends linearly on p, (ii) the derivative $|dn_s(T, p)/dT|_{T \to 0}$ depends on p slightly in the optimally and moderately doped regions ($0.10 < p \leqslant 0.16$); however, it rapidly increases with p decreasing, and (iii) the latter finding is accompanied by the linear low-temperature dependence $\Delta n_s(T) \propto (-T)$ changing to $\Delta n_s(T) \propto (-\sqrt{T})$. For optimum oxygen content the temperature dependence of the normalized imaginary part of the c-axis conductivity $\lambda_c^2(0)/\lambda_c^2(T)$ is found to be strikingly similar to that of $\lambda_{ab}^2(0)/\lambda_{ab}^2(T)$ and becomes more convex with p decreasing. $\lambda_c^{-2}(0, p)$ values are roughly proportional to the normal state conductivities $\sigma_c(T_c, p)$ along the c-axis. All these properties can be treated in the framework of d-density wave order of a pseudogap.

1. Introduction

In the past few years a lot of interest has been attracted by investigations of the nature of pseudogap states of high-T_c superconductors (HTSC) phase diagrams. This area corresponds to lower concentration p of holes per copper atom in the CuO$_2$ plane and lower critical temperatures T_c in comparison with the optimal value $p \approx 0.16$ and the maximum temperature $T_{c,max}$ of the superconducting transition. The p and T_c values in HTSCs satisfy the following empirical relationship [1]: $T_c = T_{c,max}[1 - 82.6(p - 0.16)^2]$. Currently, the origin of the pseudogap remains unclear. Proposed theoretical scenarios may be divided into two categories. One is based on the idea that the pseudogap is due to precursor superconductivity, in which pairing takes place at the pseudogap transition temperature $T^* > T_c$ but achieves coherence only at T_c. The other assumes that the pseudogap state is not related to superconductivity *per se*, but rather competes with it. This magnetic precursor scenario of the pseudogap assumes dynamical fluctuations of some kind, such as spin, charge or structural, or so-called staggered flux phase. These two scenarios treat anomalies of electronic properties

in underdoped HTSCs observed at temperatures both above T_c and in that vicinity [2–6].

In the heavily underdoped HTSC, at $T \ll T_c$ a competition between pseudogap and superconducting order parameters develops most effectively and results in the peculiarities of the superfluid density $n_s(T, p)$ as a function of T and p. It is well known that in clean BCS d-wave superconductors (DSCs) the dependence $\Delta n_s(T) \equiv n_s(T) - n_0$ is linear on temperature $T \ll T_c$: $\Delta n_s(T) \propto (-T/\Delta_0)$, where $n_0 = n_s(0)$ and $\Delta_0 = \Delta(0)$ are the superfluid density and the superconducting gap amplitude at $T = 0$. This dependence is confirmed by the measurements of the ab-plane penetration depth $\lambda_{ab}(T) = \sqrt{m^*/\mu_0 e^2 n_s(T)}$: $\Delta \lambda_{ab}(T) \propto T$ at $T < T_c/3$, where μ_0, m^* and e are the vacuum permeability, the effective mass and the electronic charge, respectively. The derivative $|dn_s(T)/dT|$ at $T \to 0$ determines the n_0/Δ_0 ratio. If thermally excited fermionic quasiparticles are the only important excitations even at $p < 0.16$, then the slope of $n_s(T)$ curves at $T \ll T_c$ is proportional to the $n_0(p)/\Delta_0(p)$ ratio: $|dn_s(T)/dT|_{T \to 0} \propto n_0(p)/\Delta_0(p)$. The measurements of $\lambda_{ab}(0)$ in underdoped HTSCs showed that the superfluid density $n_0(p) \propto \lambda_{ab}^{-2}(0)$ increases approximately linearly with $p > 0.08$, reaching its maximum value at $p \approx 0.16$ [7, 8].

With p decreasing ($p < 0.16$), the dielectric phase is being approached. Thus, the role of electron correlations and phase fluctuations becomes increasingly significant. The generalized Fermi-liquid models (GFL) allows for this through the p-dependent Landau parameter $L(p)$ [9–11] which includes $n_0(p)$. The values of $\Delta_0(p)$ and $L(p)$ determine the doping dependence of the derivative $|dn_s(T)/dT|_{T\to 0} = L(p)/\Delta_0(p)$. In [9] the ratio $L(p)/\Delta_0(p)$ does not depend on p; the model [10] predicts $L(p)/\Delta_0(p) \propto p^{-2}$. The measurements of YBa$_2$Cu$_3$O$_{7-x}$ single crystals [12] and oriented powders [13] with hole concentration $p \gtrsim 0.1$ showed that the slope of $n_s(T)$ dependences at $T \to 0$ is either slightly p-dependent [12], which agrees with [9], or diminishes with decreasing $p \leqslant 0.16$ [13], which contradicts the GFL models [9–11].

In the precursor pairing model [14, 15] of the pseudogap, based on the formation of pair electron excitations with finite momentum at $T^* > T_c$, the influence of the pseudogap order parameter on the quasiparticles spectrum at $T < T_c$ leads to a rise of $\Delta_0(p)$ and decrease of $n_0(p)$ with p decreasing. Hence, the decrease of the derivative $|dn_s(T)/dT|_{T\to 0} \propto n_0(p)/\Delta_0(p)$ is expected. The $n_s(T, p)/n_0$ dependences calculated in [15] show that their low temperature slopes decrease with underdoping. An alternative behaviour of $|dn_s(T)/dT|$ follows from the magnetic precursor d-density wave (DDW) scenario of the pseudogap [16]. In this model a DDW order parameter $W(p, T)$ is directly introduced into the quasiparticle band structure. At low energies the excitation spectrum of the DDW consists of conventional fermionic particles and holes like that of the DSC with which it competes at $p < 0.2$. The DSC gap $\Delta_0(p)$ steadily vanishes with p decreasing, whereas the sum of the zero-temperature squares $\Delta_0^2(p) + W_0^2(p)$ remains constant [17]. In the issue, the DDW model predicts a growth of the slope of $n_s(T, p)/n_0$ curves at low T and $p < 0.1$. At the same time the opening of the pseudogap influences weakly the c-axis penetration depth $\lambda_c(T, p)$ of the high-frequency field for currents running perpendicular to CuO$_2$ planes. In particular, the strong decrease of the interlayer coupling integral $t_\perp(p)$ with p decreasing [18] in YBa$_2$Cu$_3$O$_{7-x}$ dominates over effects of the DDW order on $\lambda_c(0, p)$ [19].

The present paper is aimed at the experimental verification of the above mentioned theoretical speculations.

2. Experiment

To fulfil the task, we investigated the anisotropy and evolution of the temperature dependences of microwave conductivity components in YBa$_2$Cu$_3$O$_{7-x}$ crystal under varying oxygen doping in the range $0.07 \leqslant x \leqslant 0.47$. A crystal of rectangular shape, with dimensions $1.6 \times 0.4 \times 0.1$ mm^3 was grown in a BaZrO$_3$ crucible. The measurements were made at a frequency of $\omega/2\pi = 9.4$ GHz and in the temperature range $5 \leqslant T \leqslant 200$ K. To change the oxygen content in the sample, we successively annealed the sample in air at different $T \geqslant 500\,°$C specified in table 1.

According to susceptibility measurements at the frequency of 100 kHz, the superconducting transition width amounted to 0.1 K in the optimally doped state ($x = 0.07$); however, the width increased with the increase of x, reaching

Table 1. Annealing and critical temperatures, doping parameters and penetration depths of YBa$_2$Cu$_3$O$_{7-x}$ crystal.

Annealing T (°C)	Critical T_c (K)	Doping parameters		λ values at $T = 0$		$\Delta\lambda_c(T) \propto T^\alpha$
		p	x	λ_{ab} (nm)	λ_c (µm)	α
500	92	0.16	0.07	152	1.55	1.0
520	80	0.12	0.26	170	3.0	1.1
550	70	0.106	0.33	178	5.2	1.2
600	57	0.092	0.40	190	6.9	1.3
720	41	0.078	0.47	198	16.3	1.8

4 K at $x = 0.47$. The temperatures of the superconducting transition were $T_c = 92, 80, 70, 57, 41$ K which correspond to the concentrations $p = 0.16, 0.12, 0.106, 0.092, 0.078$, respectively (table 1). Anisotropy was measured for each of the five crystal states. The whole cycle of the microwave measurements included the following:

(i) we measured the temperature dependences of the quality factor and of the frequency shift of the superconducting niobium resonator with the sample inside in the two crystal orientations with respect to the microwave magnetic field, transversal (T) and longitudinal (L);

(ii) measurements in the T orientation gave the surface resistance $R_{ab}(T)$, reactance $X_{ab}(T)$ and conductivity $\sigma_{ab}(T) = i\omega\mu_0/Z_{ab}^2(T)$ of the crystal cuprate planes in its normal and superconducting states;

(iii) measurements in the L orientation gave $\sigma_c(T)$, $X_c(T)$, $R_c(T)$.

See [20] for details of the measuring technique in optimally doped YBa$_2$Cu$_3$O$_{6.95}$ crystal.

The temperature dependences of surface impedance $Z_{ab} = R_{ab} + iX_{ab}$ components, $R_{ab}(T)$ and $X_{ab}(T)$, are shown in figure 1(a). In the normal state for each of the five crystal states we have $R_{ab}(T) = X_{ab}(T)$ which implies the validity of the normal skin-effect condition. The value of residual losses $R_{ab}(T \to 0)$ does not exceed 40 µΩ. In the case of optimum oxygen content $R_{ab}(T)$ dependence has a broad peak at $T \sim T_c/2$, which vanishes with p decreasing. At $T < T_c/3$ all $R_{ab}(T)$ curves are linear on T. In figure 1(b) we demonstrate the temperature dependences of the c-axis impedance components $R_c(T)$ and $X_c(T)$. The real and imaginary parts of the surface impedance coincide at $T > T_c$, $R_c(T) = X_c(T)$. Therefore, the resistivities $\rho_{ab}(T)$ and $\rho_c(T)$ can be found from $R_{ab}(T)$ and $R_c(T)$ curves at $T > T_c$ in figure 1, applying the standard formulae of the normal skin effect: $\rho_{ab}(T) = 2R_{ab}^2(T)/\omega\mu_0$, $\rho_c(T) = 2R_c^2(T)/\omega\mu_0$. Figure 2 shows the evolution of the dependences $\rho_{ab}(T)$ and $\rho_c(T)$ in YBa$_2$Cu$_3$O$_{7-x}$ crystal with the change of x in the temperature range $T_c < T \leqslant 200$ K.

3. Results and discussion

Figure 3 shows the low temperature sections of the measured $\lambda_{ab}(T) = X_{ab}(T)/\omega\mu_0$ curves. The linear extrapolation (dashed curves) of these dependences at $T < T_c/3$ gives the following $\lambda_{ab}(0)$ values: 152, 170, 178, 190, 198 nm for $p = 0.16, 0.12, 0.106, 0.092, 0.078$, respectively (table 1). The error in $\lambda_{ab}(T)$ is largely determined by the measurement
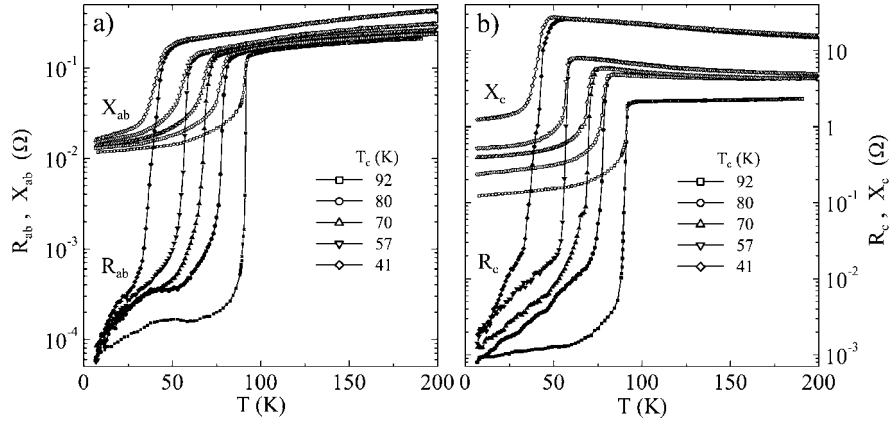
Figure 1. (a) Real $R_{ab}(T)$ (solid symbols) and imaginary $X_{ab}(T)$ (open symbols) parts of the *ab*-plane surface impedance of the five states of YBa$_2$Cu$_3$O$_{7-x}$ single crystal; (b) the components of the *c*-axis surface impedance.
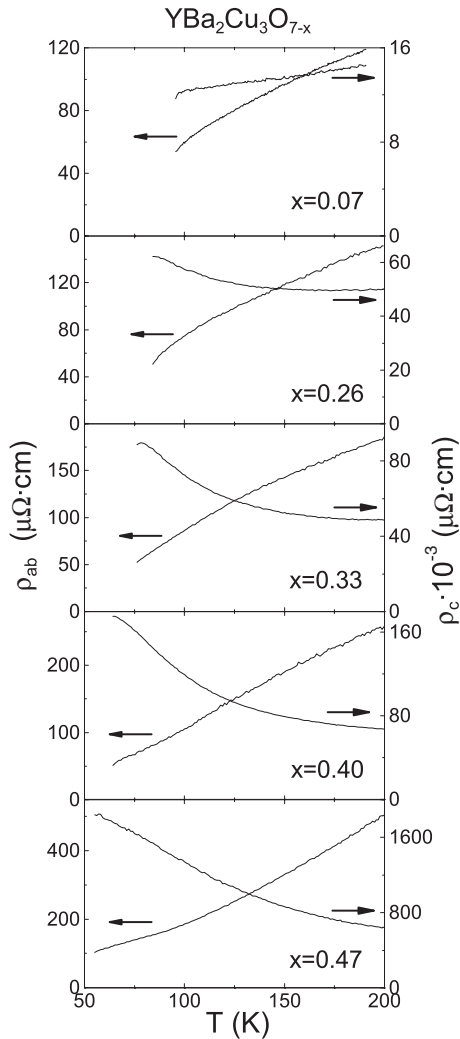
Figure 2. The evolution of the measured $\rho_{ab}(T)$ and $\rho_c(T)$ dependences in YBa$_2$Cu$_3$O$_{7-x}$ with different oxygen content.

Figure 3. Low-temperature dependences of $\lambda_{ab}(T)$ (open symbols) measured for five states of YBa$_2$Cu$_3$O$_{7-x}$ crystal with $T_c = 92$, 80, 70, 57 and 41 K. Dashed curves are linear extrapolations at $T < T_c/3$.

accuracy of the additive constant X_0, which is equal to the difference between the measured reactance shift $\Delta X_{ab}(T)$ and $R_{ab}(T)$ at $T > T_c$ [21].

As follows from figure 4, halving the concentration (i.e. from $p = 0.16$ to 0.078) results in an approximately two

times smaller $\lambda_{ab}^{-2}(0) = n_0\mu_0 e^2/m^*$ value. Similar behaviour $n_0(p) \propto p$ within the range $0.08 < p \leqslant 0.16$ was observed by other groups [7, 8]. It is easily seen that this dependence contradicts Uemura's relation $n_0(p) \propto T_c(p)$ [22]. The naive linear extrapolation of the dashed curve in figure 4 at $p < 0.08$ leads to a nonphysical result: $n_0(p)$ is finite at vanishing p. To the best of our knowledge there is no data of superfluid density measurements in HTSC at $p < 0.08$. As for theoretical predictions, n_0 linearity on p extends down to $p = 0$ in the model [9], while in the DDW scenario [17, 23] it exists in the underdoped range of the phase diagram where the DSC order parameter grows from zero to its maximal value, moreover $n_0(p)$ is nonzero as $\Delta_0(p)$ vanishes (figure 1 from [23]). The latter agrees with our data.

In figure 4 we also show the slopes $|d\lambda_{ab}^{-2}(T)/dT|_{T\to 0} \propto |dn_s(T)/dT|_{T\to 0}$ of $\lambda_{ab}^{-2}(T)$ curves obtained from $\lambda_{ab}(T)$ dependences at $T < T_c/3$. The value of $|d\lambda_{ab}^{-2}(T)/dT|$ changes slightly at $0.1 < p \leqslant 0.16$ in accordance with [9]. However, it grows drastically at $p \lesssim 0.1$, i.e. the $\lambda_{ab}^{-2}(T)$ slope increases 2.5 times with p decreasing from 0.12 to 0.08. The $|d\lambda_{ab}^{-2}(T)/dT| \propto p^{-2}$ dependence [10] is shown by the
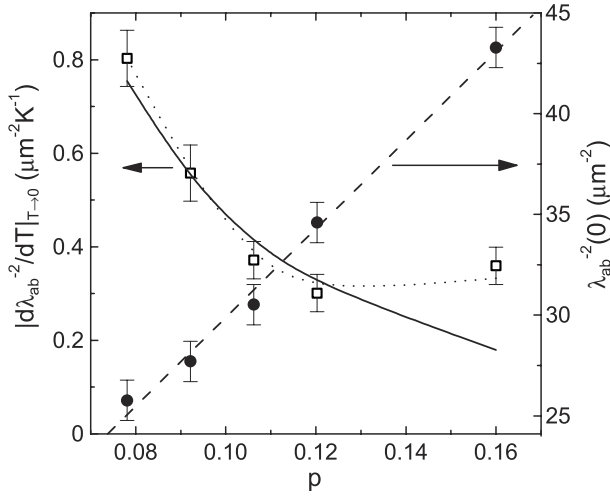
Figure 4. The values of $\lambda_{ab}^{-2}(0) = n_s(0)\mu_0 e^2/m^*$ (right scale) and slopes $|d\lambda_{ab}^{-2}(T)/dT|_{T\to 0} = \mu_0 e^2/m^*|dn_s(T)/dT|_{T\to 0}$ (left scale) as a function of doping $p = 0.16 - \sqrt{(1 - T_c/T_{c,max})/82.6}$ with $T_{c,max} = 92$ K in YBa$_2$Cu$_3$O$_{7-x}$. Error bars correspond to experimental accuracy. The dashed and dotted curves guide the eye. The solid curve is the $|dn_s(T)/dT| \propto p^{-2}$ dependence.
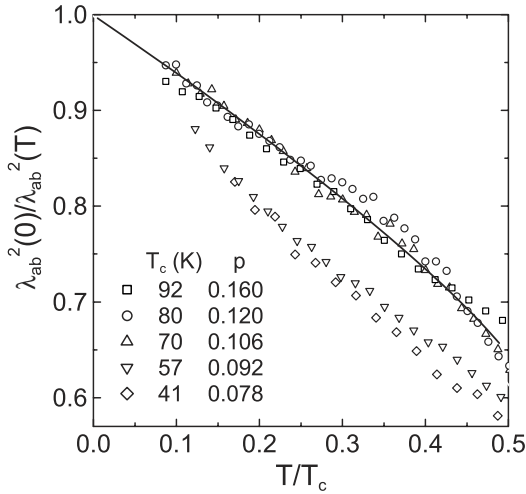
Figure 5. The measured dependences of $\lambda_{ab}^2(0)/\lambda_{ab}^2(T) = n_s(T)/n_s(0)$ at $T < T_c/2$ in YBa$_2$Cu$_3$O$_{7-x}$ with different doping. The solid curve is the $\lambda_{ab}^2(0)/\lambda_{ab}^2(T)$ dependence in the BCS d-wave superconductor (DSC).

solid curve in figure 4 and roughly fits the data at $p \leqslant 0.12$. The dotted curve drawn through $|d\lambda_{ab}^{-2}(T)/dT|$ experimental points in figure 4 qualitatively agrees with the behaviour of this quantity in the DDW model [17, 23].

The temperature dependence of the superfluid density $n_s(T)$ at low T in the heavily underdoped YBa$_2$Cu$_3$O$_{7-x}$ proves to be one more check-up of the DDW scenario of the pseudogap. $\lambda_{ab}^2(0)/\lambda_{ab}^2(T) = n_s(T)/n_0$ dependences obtained from the data in figure 3 are shown in figure 5 for different p values. The solid curve represents the DSC result. The evident peculiarities in figure 5 are the concavity of $n_s(T)/n_0$ curves corresponding to the heavily underdoped states ($p = 0.078$ and 0.092) and their deviation from DSC and the curves for $p = 0.16, 0.12, 0.106$. This behaviour of the superfluid density $n_s(T)/n_0$ contradicts the conclusions of
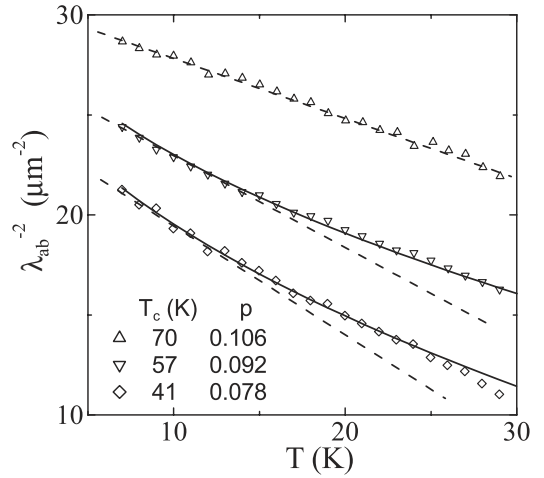
Figure 6. Comparison of experimental $\lambda_{ab}^{-2}(T) \propto n_s(T)$ curves (symbols) with linear $\Delta\lambda_{ab}^{-2}(T) \propto (-T)$ (dashed lines) and root $\Delta\lambda_{ab}^{-2}(T) \propto (-\sqrt{T})$ (solid curves) dependences for moderately doped ($p = 0.106$, $x = 0.33$) and heavily underdoped ($p = 0.092$, $x = 0.40$; $p = 0.078$, $x = 0.47$) YBa$_2$Cu$_3$O$_{7-x}$.

the precursor pairing model [15], but agrees with the DDW scenario [17]. The latter predicts $n_s(T)$ linearity in a wide range of temperatures for the optimally and moderately doped samples. However, for the heavily underdoped samples the situation is quite different. Though in the asymptotically low-temperature regime the suppression of the superfluid density is linear on temperature, there is an intermediate temperature range over which the suppression actually behaves as $\sqrt{T}$. Actually, in the intermediate temperature range $0.1T_c < T \lesssim 0.5T_c$ the experimental $n_s(T)$ curves in YBa$_2$Cu$_3$O$_{6.60}$ and YBa$_2$Cu$_3$O$_{6.53}$ with $p < 0.1$ are not linear but similar to $\sqrt{T}$-dependences. This is confirmed by figure 6, where the measured $\lambda_{ab}^{-2}(T) \propto n_s(T)$ dependences are compared with $\sqrt{T}$-dependences $\Delta\lambda_{ab}^{-2}(T) = -3\sqrt{T}$ (λ_{ab} and T are expressed in μm and K) in YBa$_2$Cu$_3$O$_{6.60}$ ($p = 0.092$) and $\Delta\lambda_{ab}^{-2}(T) = -3.5\sqrt{T}$ in YBa$_2$Cu$_3$O$_{6.53}$ ($p = 0.078$). Dashed linear curves in figure 6 correspond to the linear at $T < T_c/3$ dependences of $\lambda_{ab}(T)$ presented in figure 3 and extended to higher temperatures.

It is also interesting to note that these deviations of $\Delta\lambda_{ab}^{-2}(T)$ in YBa$_2$Cu$_3$O$_{6.60}$ and YBa$_2$Cu$_3$O$_{6.53}$ are accompanied by inflection of the resistivity $\rho_{ab}(T)$ curves in the normal state of these samples. These inflections are seen at two lower $\rho_{ab}(T)$ curves in figure 2 around $T \sim 100$ K. One more feature of the curves in figure 2 is that only the optimally doped YBa$_2$Cu$_3$O$_{6.93}$ shows that both dependences $\rho_{ab}(T)$ and $\rho_c(T)$ have a metallic behaviour, and the ratio ρ_c/ρ_{ab} approaches the anisotropy of effective masses of charge carriers $m_c/m_{ab} = \lambda_c^2(0)/\lambda_{ab}^2(0)$ in a 3D London superconductor, of which type YBa$_2$Cu$_3$O$_{6.93}$ belongs to. The other states of YBa$_2$Cu$_3$O$_{7-x}$ have the resistivity $\rho_c(T)$ increase with the decrease of temperature, so that decrease of carrier concentration in YBa$_2$Cu$_3$O$_{7-x}$ crystal results in the crossover from the Drude c-axis conductivity to the tunnelling one [24]. The evolution of the temperature dependences of $\rho_c(T)$ with doping correlates with those of the c-axis penetration depth $\lambda_c(T)$. Solid symbols of figure 7 show the dependences $\lambda_c^2(0)/\lambda_c^2(T)$ at
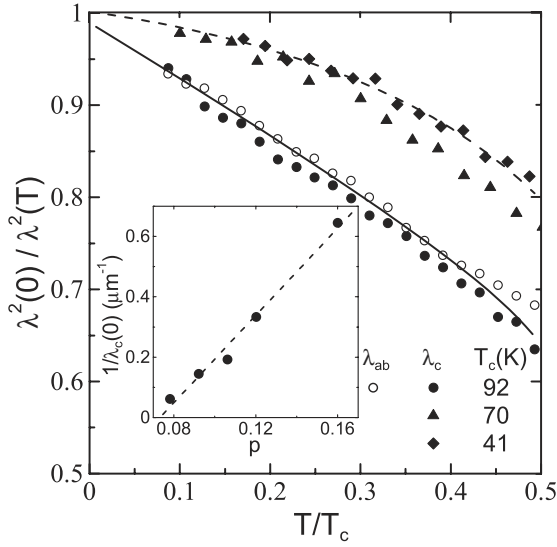
Figure 7. The dependence $\lambda_{ab}^2(0)/\lambda_{ab}^2(T)$ (open symbols) in YBa$_2$Cu$_3$O$_{6.93}$ and $\lambda_c^2(0)/\lambda_c^2(T)$ (full symbols) measured for three states of the YBa$_2$Cu$_3$O$_{7-x}$ crystal with T_c = 92, 70 and 41 K. Solid and dashed curves stand for the dependences $\lambda_c^2(0)/\lambda_c^2(T)$ calculated in [25] for YBa$_2$Cu$_3$O$_{7-x}$ with different oxygen deficiency. The inset shows $1/\lambda_c$ at $T = 0$ as a function of doping p.

$T \leqslant T_c/2$ for YBa$_2$Cu$_3$O$_{7-x}$ states with T_c = 92, 70 and 41 K. Table 1 contains the values of the penetration depth $\lambda_c(0)$ at $T = 0$ and the exponents α in the measured $\lambda_c(T) - \lambda_c(0) = \Delta\lambda_c(T) \propto T^\alpha$ dependences at $T \leqslant T_c/3$. The peculiarity of the optimally doped state YBa$_2$Cu$_3$O$_{6.93}$ is a good coincidence of $\lambda_{ab}^2(0)/\lambda_{ab}^2(T)$ (open circles in figure 7) and $\lambda_c^2(0)/\lambda_c^2(T)$ temperature dependences. With the decrease of p the temperature dependence of $\lambda_c^2(0)/\lambda_c^2(T)$ becomes substantially weaker than that of $\lambda_{ab}^2(0)/\lambda_{ab}^2(T)$. Model [25] associates the reduction in the low-T slope of $\lambda_c^2(0)/\lambda_c^2(T)$ curves and the appearance of semiconducting-like temperature dependence of $\rho_c(T)$ with a decrease of the interlayer coupling in the crystal. The dashed curve in figure 7 represents numerical results [25] for this case. On the other hand, in the optimally doped YBa$_2$Cu$_3$O$_{6.93}$ the interlayer coupling is strong and quasiparticle transport along the c-axis becomes identical to the one in the anisotropic 3D superconductor [26]. The solid curve in figure 7 is $\lambda_c^2(0)/\lambda_c^2(T)$ dependence, calculated in [25] for this particular case. So, the low-T dependences of $\lambda_c(T)$ are well described without taking pseudogap effects into consideration. Let us consider now their possible manifestations in the doping dependence of the c-axis penetration depth.

From the inset to figure 7 it follows that the reciprocal value of the zero-temperature penetration depth $1/\lambda_c(0, p)$ is roughly linear on p. Note that it vanishes at $p \approx 0.07$ which is near the value where T_c does too [23, 27]. There are several theoretical models [25, 28] and experimental confirmations [29] of the direct proportionality of $\lambda_c^{-2}(0)$ to the c-axis conductivity $\sigma_c(T_c)$ in HTSC. In the simplest theory this correlation is caused by the $\lambda_c^{-2} \propto J_c$ relation, where J_c is the c-axis critical current in the d-wave superconductor with anisotropic interlayer scattering and weak interlayer coupling. The value of $J_c(0)$ is determined by both the superconducting gap Δ_0 and conductivity $\sigma_c(T_c)$. The symbols in the lower
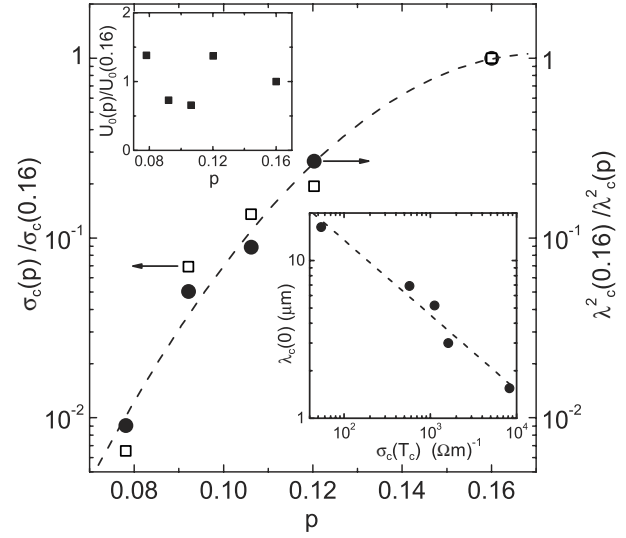
Figure 8. Doping dependences of $\lambda_c^2(p)/\lambda_c^2(0.16)$ at $T = 0$ and $\sigma_c(p)/\sigma_c(0.16)$ at $T = T_c$. Their ratio $U_0(p)/U_0(0.16)$ is shown in the upper inset. The lower inset is $\lambda_c(0)$ versus $\sigma_c(T_c)$ plot.

inset to figure 8 show our data fitted by the dashed curve $\log \lambda_c(0)$ (μm) = $-0.5 \log \sigma_c(T_c)$ (Ω^{-1} m^{-1}) + 2.1. The latter constant defines a proportionality factor $U_0(p)$ in the $\lambda_c^{-2}(0, p) = U_0(p)\,\sigma_c(T_c, p)$ relation. In the framework of the DDW model the value of $U_0(p)$ is determined by the doping dependences of $\Delta_0(p)$, $W_0(p)$ and chemical potential $\mu(p)$. As is shown in [19] the opening of the DDW gap can lead to an increase as well as to a decrease of $U_0(p)$. This depends on the position of the Fermi surface with respect to the DDW gap, but in any case $U_0(p)$ changes less than twice in the whole range of doping. The values of $\lambda_c^2(0.16)/\lambda_c^2(p)$ at $T = 0$ and $\sigma_c(p)/\sigma_c(0.16)$ at $T = T_c$ are shown in figure 8. Their ratio $U_0(p)/U_0(0.16)$ is demonstrated in the upper inset to figure 8. This weak doping dependence indicates that the contribution of the interlayer coupling integral $t_\perp(p) \propto \sigma_c(T_c, p)$ into $\lambda_c(0, p)$ is dominant.

Thus, the four main experimental observations of this paper are:

(i) linear dependence of $n_0(p)$ in the range $0.078 \leqslant p \leqslant 0.16$,

(ii) drastic increase of the low-temperature $n_s(T)$ slope at $p < 0.1$,

(iii) the deviation of $\Delta n_s(T)$ dependence from universal BCS behaviour $\Delta n_s(T) \propto (-T)$ at $T < T_c/2$ towards $\Delta n_s(T) \propto (-\sqrt{T})$ with decreasing $p < 0.1$, and

(iv) very weak influence of the pseudogap on the low-T and doping dependences of the c-axis penetration depth. All these facts evidence the DDW scenario of electronic processes in underdoped HTSC. Nevertheless, the measurements of $\lambda_{ab}(T)$ and $\lambda_c(T)$ at lower temperatures and in the high-quality samples with smaller carrier density are necessary for an ultimate conclusion.

Acknowledgments

References

[1] Tallon J L *et al* 1995 *Phys. Rev.* B **51** 12911
[2] Timusk T and Statt B 1999 *Rep. Prog. Phys.* **62** 61
[3] Tallon J L and Loram J W 2001 *Physica* C **349** 53
[4] Sadovskii M V 2001 *Usp. Fiz. Nauk* **171** 539
    Sadovskii M V 2001 *Phys.—Usp.* **44** 515 (Engl. Transl.)
[5] Norman M R and Pépin C 2003 *Rep. Prog. Phys.* **66** 1547
[6] Pines D 2000 *Physica* C **341–348** 59
    Schmalian J, Pines D and Stojkovic B 1999 *Phys. Rev.* B **60** 667
[7] Loram J W *et al* 2001 *J. Phys. Chem. Solids* **62** 59
[8] Bernhard C *et al* 2001 *Phys. Rev. Lett.* **86** 1614
[9] Lee P A and Wen X-G 1997 *Phys. Rev. Lett.* **78** 4111
[10] Millis A J, Girvin S M, Ioffe L B and Larkin A I 1998 *J. Phys. Chem. Solids* **59** 1742
[11] Ioffe L B and Millis A J 2002 *J. Phys. Chem. Solids* **63** 2259
[12] Bonn D A *et al* 1996 *Czech. J. Phys.* **46** 3195
[13] Panagapoulos C, Cooper J R and Xiang T 1998 *Phys. Rev.* B **57** 13422
[14] Kostzin I *et al* 2001 *Phys. Rev.* B **61** 11662
[15] Levin K *et al* 2002 *J. Phys. Chem. Solids* **63** 2233
[16] Chakravarty S *et al* 2001 *Phys. Rev.* B **63** 094503
[17] Tewari S *et al* 2001 *Phys. Rev.* B **64** 224516
[18] Nyhus P *et al* 1994 *Phys. Rev.* B **50** 13898
[19] Kim W *et al* 2002 *Phys. Rev.* B **65** 064502
[20] Nefyodov Yu A *et al* 2003 *Phys. Rev.* B **67** 144504
[21] Trunin M R, Nefyodov Yu A and Shevchun A F 2004 *Phys. Rev. Lett.* **92** 067006
[22] Uemura Y J 1997 *Physica* C **282–287** 194
[23] Wang Q-H, Han J H and Lee D-H 2001 *Phys. Rev. Lett.* **87** 077004
[24] Trunin M R and Nefyodov Yu A 2003 *Pis. Zh. Eksp. Teor. Fiz.* **77** 696
    Trunin M R and Nefyodov Yu A 2003 *JETP Lett.* **77** 592 (Engl. Transl.) (*Preprint* cond-mat/0306158)
[25] Radtke R J, Kostur V N and Levin K 1996 *Phys. Rev.* B **53** R522
[26] Xiang T, Panagapoulos C and Cooper J R 1998 *Int. J. Mod. Phys.* B **12** 1007
[27] Nayak C and Pivovarov E 2002 *Phys. Rev.* B **66** 064508
[28] Hirschfeld P J, Quinlan S M and Scalapino D J 1997 *Phys. Rev.* B **55** 12742
    Chakravarty S, Kee H-Y and Abrahams E 1999 *Phys. Rev. Lett.* **82** 2366
    Ohashi Y 2000 *J. Phys. Soc. Japan* **69** 659
[29] Basov D N *et al* 1994 *Phys. Rev.* B **50** 3511
    Kirtley J R *et al* 1998 *Phys. Rev. Lett.* **81** 2149
    Dordevic S V *et al* 2002 *Phys. Rev.* B **65** 134511